

SCIENTIFIC REPORTS



OPEN

Ubiquitin Ligase Huwe1 Modulates Spermatogenesis by Regulating Spermatogonial Differentiation and Entry into Meiosis

Rohini Bose^{1,2}, Kai Sheng^{1,2}, Adel R. Moawad^{1,3,7}, Gurpreet Manku^{1,2,4}, Cristian O'Flaherty^{1,3,4}, Teruko Taketo^{1,3,5,6}, Martine Culty^{1,2,8}, Kin Lam Fok^{1,2,9,10} & Simon S. Wing^{1,2}

Spermatogenesis consists of a series of highly regulated processes that include mitotic proliferation, meiosis and cellular remodeling. Although alterations in gene expression are well known to modulate spermatogenesis, posttranscriptional mechanisms are less well defined. The ubiquitin proteasome system plays a significant role in protein turnover and may be involved in these posttranscriptional mechanisms. We previously identified ubiquitin ligase Huwe1 in the testis and showed that it can ubiquitinate histones. Since modulation of histones is important at many steps in spermatogenesis, we performed a complete characterization of the functions of Huwe1 in this process by examining the effects of its inactivation in the differentiating spermatogonia, spermatocytes and spermatids. Inactivation of Huwe1 in differentiating spermatogonia led to their depletion and formation of fewer pre-leptotene spermatocytes. The cell degeneration was associated with an accumulation of DNA damage response protein γ H2AX, impaired downstream signalling and apoptosis. Inactivation of Huwe1 in spermatocytes indicated that Huwe1 is not essential for meiosis and spermiogenesis, but can result in accumulation of γ H2AX. Collectively, these results provide a comprehensive survey of the functions of Huwe1 in spermatogenesis and reveal Huwe1's critical role as a modulator of the DNA damage response pathway in the earliest steps of spermatogonial differentiation.

Spermatogenesis is a tightly regulated process that ensures the successful production of millions of genetically unique haploid spermatozoa each day. Occurring within the seminiferous epithelium in tubules of the testis, spermatogenesis is sustained by a small population of undifferentiated spermatogonial progenitors which include the spermatogonial stem cells¹. Throughout adulthood, some of these progenitors become committed to differentiation. This initiation of differentiation takes place asynchronously throughout the testis to assure continuous production of sperm. However, at any specific location in the seminiferous epithelium, differentiation is initiated in a precisely timed manner, which in the mouse occurs every 8.6 days. Retinoic acid, through the induction of the *Stra8* gene, is the critical signal for inducing this transition to A₁ spermatogonia, the earliest differentiated spermatogonia². Subsequently, the A₁ spermatogonia proceed through six rounds of synchronous cell divisions in rodents (A₂, A₃, A₄, Intermediate (In), Type B spermatogonia) to finally give rise to primary or pre-leptotene spermatocytes^{3,4} in early meiosis. During meiotic prophase I, homologous chromosomal recombination occurs which is critical for creating the genetically diverse spermatids. The induction of *Spo11* recombinase plays a vital role in the generation of double strand breaks in this process⁵. Following the two rounds of meiotic division, the

¹The Research Institute of the McGill University Health Centre, Montréal, Québec, Canada. ²Department of Medicine, McGill University, Montréal, Québec, Canada. ³Department of Surgery, McGill University, Montréal, Québec, Canada. ⁴Department of Pharmacology and Therapeutics, McGill University, Montréal, Québec, Canada. ⁵Department of Obstetrics and Gynecology, McGill University, Montréal, Québec, Canada. ⁶Department of Biology, McGill University, Montréal, Québec, Canada. ⁷Department of Theriogenology, Faculty of Veterinary Medicine, Cairo University, Giza, Egypt. ⁸Present address: Dept. of Pharmacology, University of Southern California, Los Angeles, California, USA. ⁹Present address: Epithelial Cell Biology Research Center, School of Biomedical Sciences, The Faculty of Medicine, The Chinese University of Hong Kong, Sha Tin, Hong Kong. ¹⁰Present address: Shenzhen Research Institute, The Chinese University of Hong Kong - Shenzhen, Shenzhen, China. Correspondence and requests for materials should be addressed to S.S.W. (email: simon.wing@mcgill.ca)

haploid spermatids undergo a process of cellular remodeling and condensation, referred to as spermiogenesis. As part of this process, histones are removed and replaced by protamines, which enable tighter packing of the chromatin⁶. Defects in spermatogenesis lead to azoospermia in humans^{7,8} and so it is important to acquire a comprehensive understanding of the molecular mechanisms underlying spermatogonial differentiation. There are plentiful studies describing the transcriptional programs controlling spermatogonial differentiation^{9–15}. However, the post-transcriptional regulation underlying spermatogonial differentiation remains largely unknown.

The ubiquitin system has both proteolytic and non-proteolytic functions in spermatogenesis¹⁶. The system functions by activating and transferring ubiquitin to proteins by a three-enzyme cascade: the E1 or the ubiquitin-activating enzyme, E2 or the ubiquitin-conjugating enzyme and E3 or the ubiquitin ligase. Ubiquitin ligases are responsible for substrate selectivity and specificity and mediate the final step of covalently tagging proteins with the ubiquitin moiety. Huwe1 is a ubiquitin ligase that was first identified by our laboratory as a testis E3 that can ubiquitinate all core histones *in vitro*¹⁷. Since regulation of histones plays an important role in many steps of spermatogenesis, we inactivated the enzyme specifically in the germ cells to characterize its functions. Inactivation of Huwe1 in the gonocytes leads to a defect in establishment and maintenance of spermatogonia resulting in a Sertoli cell-only phenotype in the adult testis and infertility¹⁸. Cell degeneration in the knockout testis occurs through mitotic catastrophe associated with a hyperactivation of the DNA damage response pathway (DDR) attributed to the accumulation of both histone H2AX and its phosphorylated isoform γ H2AX in undifferentiated spermatogonia¹⁸.

Since loss of Huwe1 in gonocytes results in depletion of spermatogonia starting as early as 6 days post partum (dpp), we were unable to study functions of the ligase beyond this point. To explore for additional roles of Huwe1, we inactivated the enzyme using Cre-recombinase driven by the *Stra8* promoter which turns on in type A₁ spermatogonia and is active up to the pre-leptotene spermatocytes¹⁹ and by the *Spo11* promoter which is activated in spermatocytes that have initiated meiosis²⁰. With this approach, we show that indeed Huwe1 has critical roles in spermatogonial differentiation leading up to meiosis.

Results

Inactivation of Huwe1 in differentiating spermatogonia leads to an arrest in spermatogenesis.

To identify roles for Huwe1 in germ cells committed to the spermatogenic program, we inactivated Huwe1 in the differentiating spermatogonia by crossing conditional *Huwe1* knockout female mice (*Huwe1*^{lox/lox})²¹ with males expressing a *Stra8-Cre* transgene hemizygotously¹⁹. The *Stra8* gene is activated directly by retinoic acid and is one of the earliest genes induced in differentiating spermatogonia and therefore a marker of A₁ spermatogonia²². Since *Huwe1* is an X-linked gene, all the males obtained from this cross were either the genotype *Huwe1*^{lox/Y} (hereafter referred to as WT) or *Huwe1*^{-Y} *Stra8-Cre* (hereafter referred to as *Stra8-Cre* KO). Excision of the lox-P flanked region was confirmed by RT-PCR of whole testes RNA (Supplementary Figure 1). A fertility assay comparing the two genotypes revealed that the *Stra8-Cre* KO males had similar copulatory behavior, measured as the frequency of vaginal plugging (Fig. 1a). However, they were unable to sire any litters. In addition, the average weight of their adult testes was only 30% of the WT (Fig. 1b). Examination of histological sections of testes revealed that there was significant loss of differentiating spermatogonia, spermatocytes and extensive loss of spermatids in the tubules (Fig. 1c). The epididymis of the *Stra8-Cre* KO had only a few sperm (Fig. 1d) with the average caudal sperm number being 3% of that seen in the WT (Fig. 1e). Collectively, these results indicate that Huwe1 activity in the differentiating spermatogonial population is crucial for male fertility, its inactivation leading to a developmental arrest early in spermatogenesis.

Huwe1 is a critical regulator of spermatogonial differentiation. During spermatogenesis, seminiferous tubules transition through multiple stages, each constituting different sets of cellular associations. As this process occurs asynchronously amongst tubules, a typical cross section of a testis will present tubules in different stages of spermatogenesis. Since staging of tubules depends on analysis of structural features of the acrosome, nucleus and position of spermatids, its accuracy is limited in scenarios such as the *Stra8-Cre* KO testis where spermatids are absent. To sharpen the resolution of stage-specific defects occurring in the KO testis, we synchronized the tubules to ensure simultaneous division and differentiation of the germ cells with a strategy previously described by Hogarth *et al.*²³. WT and *Stra8-Cre* KO mice were fed with WIN 18,446, an inhibitor of retinaldehyde dehydrogenase, an enzyme that is essential for retinoic acid (RA) synthesis. This treatment resulted in the accumulation of undifferentiated spermatogonia. The mice were then given an injection of retinoic acid to initiate differentiation simultaneously in all the tubules. The animals were sacrificed 48 days post RA injection (dpRA), a time-point at which we expected the tubules to have completed the first wave of spermatogenesis and be in Stage VIII containing specific cell types namely, the A_s, A_{pr} (undifferentiated spermatogonia), A₁ spermatogonia, pre-leptotene and pachytene spermatocytes and step 8 and 16 spermatids. The testis sections were stained with antibody against *Stra8* (expressed from A₁ spermatogonia to pre-leptotene spermatocytes) to identify the spermatogonia (located adjacent to the basement membrane of the tubules) and the pre-leptotene spermatocytes (located away from the basement membrane)²² (Fig. 2a). The *Stra8-Cre* KO testis had fewer *Stra8*⁺ pre-leptotene spermatocytes, which indicated that there was a defect in the process of spermatogonial differentiation. This was confirmed by measuring the expression of markers of spermatogonial differentiation (*Stra8*, *Dazl*, *Sohlh2*) by Q-PCR, which were markedly decreased in the *Stra8-Cre* KO testis (Fig. 2b).

Since these results suggested a defect in spermatogonial differentiation, we focused on this process by sacrificing the animals at 8 dpRA when the WT testis tubules will contain either pre-leptotene or leptotene spermatocytes from the first round of differentiation or A₁ or A₂ spermatogonia from the second round of differentiation. Hematoxylin and eosin staining of these sections showed a clear loss of pre-leptotene/leptotene spermatocytes (germ cells located away from the basement membrane) in the tubules of the *Stra8-Cre* KO testis (Fig. 2c). To identify the germ cells more precisely, we stained the sections with antibody against *Stra8*,

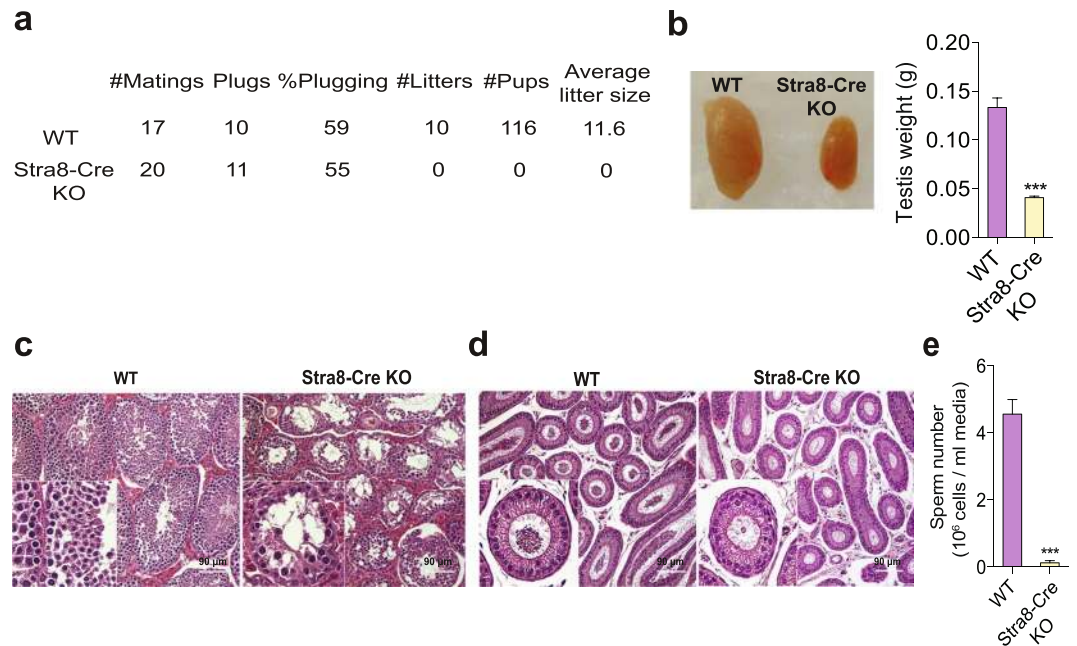


Figure 1. Inactivation of *Huwe1* in the differentiating spermatogonia leads to an arrest in spermatogenesis. **(a)** Inactivation of *Huwe1* in the differentiating spermatogonia leads to infertility. WT and Stra8-Cre KO ($n = 5$) male mice were mated with CD1 females for 4 consecutive weeks. The females were changed every week. Indicated are the frequency of vaginal plugging, number of litters sired and the average litter size. **(b)** Adult Stra8-Cre KO mice have smaller testes than WT mice. Representative images (left panel) and weights (right panel) of testis from WT ($n = 9$) and Stra8-Cre KO ($n = 10$) mice. **(c)** Arrested spermatogenesis in the Stra8-Cre KO testis. Hematoxylin and eosin stained testicular tissue sections from adult (4 month old) WT and Stra8-Cre KO testes. Scale bar = $90\ \mu\text{m}$. **(d)** Few sperm in the Stra8-Cre KO epididymis. Hematoxylin and eosin stained caput (head of the epididymis) tissue sections from adult WT and Stra8-Cre KO. Scale bar = $90\ \mu\text{m}$. **(e)** Low sperm number in the Stra8-Cre KO mice. Measurement of sperm number in the cauda (tail of the epididymis) of WT and Stra8-Cre KO ($n = 5$) mice. Data are shown as mean \pm SEM. Student's t-test. *** $p < 0.001$.

which labels spermatogonia and pre-leptotene spermatocytes, but not leptotene spermatocytes (Fig. 2d). There was a significant decrease in the average number of Stra8 + cells in the Stra8-Cre KO testis. While there was no difference in spermatogonia (Stra8 + cells located adjacent to the basement membrane of the tubules), the number of pre-leptotene spermatocytes (Stra8 + cells located away from the basement membrane of the tubules) was significantly lower in the Stra8-Cre KO testis (Fig. 2d). Taken together, these results show that the inactivation of *Huwe1* leads to disrupted spermatogonial differentiation and hence perturbed formation of pre-leptotene spermatocytes.

Inactivation of *Huwe1* leads to a defect in entry into meiosis. Pre-leptotene spermatocytes undergo a single round of DNA replication, an essential process for the subsequent reductive division occurring in prophase I of meiosis²⁴. Since recent work in our laboratory has shown *Huwe1* to be important for the mitotic reentry of gonocytes¹⁸, we asked if it regulates this developmental transition as well. To this end, we injected BrdU at 7 dpRA and sacrificed the mice 24 hr later. Immunofluorescence staining for BrdU and Stra8 was performed to identify the proliferating differentiating spermatogonia and pre-leptotene spermatocytes (Fig. 3a). Quantification revealed that the proportion of pre-leptotene spermatocytes incorporating BrdU was approximately 50% lower in the Stra8-Cre KO testis compared to the WT. There was no significant difference in the proportion of differentiating spermatogonia that were incorporating BrdU between the two groups (Fig. 3a). In addition, qPCR measurement of markers of early meiosis (*Spo11*, *Smc1b*, *Sycp1*, *Sycp3*) revealed a significant down-regulation of the expression of these genes (Fig. 3b). Staining with SYCP3 (a commonly used marker to identify different types of spermatocytes in meiotic prophase I)²⁵ confirmed that the Stra8-Cre KO testis had fewer leptotene spermatocytes (Fig. 3c). Taken together, these experiments revealed *Huwe1*'s critical role as a regulator of proliferation during commitment to meiosis.

Inactivation of *Huwe1* in the differentiating spermatogonia leads to an activation of the DDR and cell death through apoptosis. Our previous studies on the role of *Huwe1* in undifferentiated spermatogonia showed that the enzyme is important for regulating H2AX levels. *Huwe1* deficiency in these cells leads to elevated H2AX and a hyperactivation of the DDR resulting in mitotic catastrophe¹⁸. We therefore asked if *Huwe1* performs a similar function during the process of spermatogonial differentiation. To this end, we isolated testes from WT and Stra8-Cre KO mice at 10 dp, a time point at which we expected to capture all the differentiating spermatogonia and pre-leptotene spermatocytes with the most advanced cell type being the leptotene

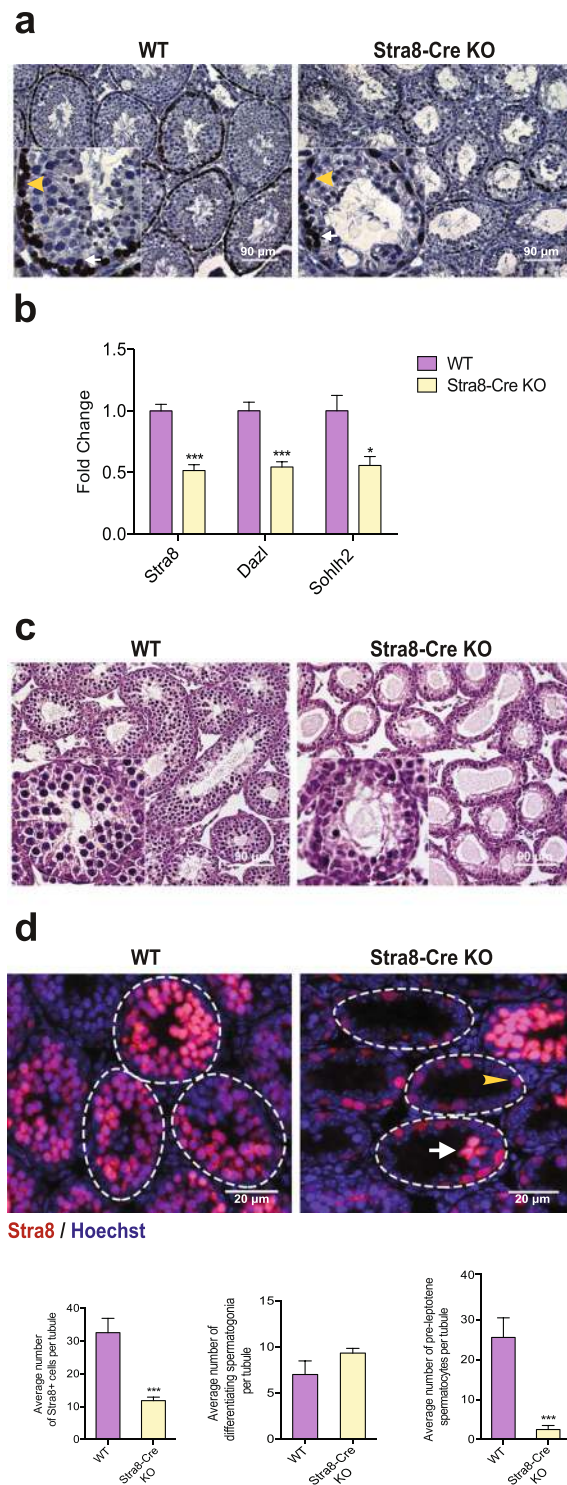


Figure 2. Huw1 is a critical regulator of spermatogonial differentiation. (a) Disrupted formation of pre-leptotene spermatocytes in synchronized Stra8-Cre KO testis 48 days post retinoic acid (dpRA) adult testes. Representative immunohistochemical images from WT and Stra8-Cre KO testis sections stained for Stra8. Pre-leptotene spermatocytes are identified based on their Stra8 positivity and location in the seminiferous tubules away from the basement membrane. The yellow arrowhead indicates an A₁ differentiating spermatogonia and the white arrow indicates a pre-leptotene spermatocyte. Scale bar = 90 μm. (b) Expression of markers for differentiating spermatogonia is decreased in synchronized Stra8-Cre KO 48 dpRA adult testes. Q-PCR analysis of markers of differentiating spermatogonia (*Stra8*, *Dazl*, *Sohlh2*) in the WT (n = 5) and Stra8-Cre KO (n = 6) testis. (c) Loss of pre-leptotene/leptotene spermatocytes (germ cells located away from the basement membrane) in synchronized Stra8-Cre KO 8 dpRA tubules. Hematoxylin and eosin stained testicular tissue sections from neonatal WT and Stra8-Cre KO mice. Scale bar = 90 μm. (d) Few pre-leptotene spermatocytes in the synchronized Stra8-Cre KO 8 dpRA testis. Representative immunofluorescence images of synchronized

WT and Stra8-Cre KO testis stained for Stra8 (red) (top panel). Stra8+ cells at the basement membrane of tubule are A₁ differentiating spermatogonia (arrowhead); Stra8+ cells away from the basement membrane are pre-leptotene spermatocytes (arrow). Quantification from the images (bottom panel). WT, n = 5 (135 tubules) Stra8-Cre KO, n = 7 (271 tubules). Scale bar = 20 μm. Data are shown as mean ± SEM. Student's t-test. ***p < 0.001, *p < 0.05.

spermatocytes²⁶. We stained the sections for γH2AX and Stra8 (Fig. 4a) and found an increased proportion of differentiating spermatogonia and pre-leptotene spermatocytes in the Stra8-Cre KO testis showing intense γH2AX foci. Activation of the ATM arm of the DDR pathway, upstream of H2AX, was further confirmed by staining for another of its targets, pCHK2 (Fig. 4b). To examine events downstream of the recruitment of γH2AX, we stained for ubiquitinated foci which reflects propagation of the DDR. Surprisingly, the excess clustering of γH2AX did not lead to significant staining for ubiquitin (Supplementary Figure 3) of the γH2AX foci, suggesting a defect in the DDR immediately downstream of γH2AX in the KO cells. Testes from 6 dpp mice where Huwe1 had been inactivated using Cre recombinase driven by Dxd4 promoter, were used as a positive control for observing the accumulation of ubiquitinated foci¹⁸. Although the inactivation of Huwe1 in gonocytes does not lead to increased apoptosis but death via mitotic catastrophe, the DDR is well recognized to promote apoptosis in other cell contexts²⁷. Therefore, we explored whether the activation of the DDR pathway in the Stra8-Cre KO testis led to increased levels of apoptosis. Indeed, we found that there was a significant increase in apoptosis in the 8 dpRA Stra8-Cre KO testis as measured by the TUNEL assay of DNA fragmentation (Fig. 4c). We confirmed this result by staining the same sections with cleaved, activated caspase 3 (Fig. 4d), a downstream effector enzyme in the apoptotic cascade^{28,29}. Co-staining for Tra98 (a germ cell marker) and cleaved caspase 3 showed that this increase in apoptosis in the Stra8-Cre KO tubules was not due to an increase in apoptosis of Sertoli cells, as approximately 68% of the apoptotic cells in the Stra8-Cre KO tubules were germ cells compared to 46% in the WT, as determined by double staining for Tra98 (a germ cell marker) and cleaved caspase 3 (data not shown). To explore whether this apoptosis was mediated through activation of p53, we stained the testis sections with anti-phosphorylated p53 antibody. There was no significant colocalization of p53 to the nuclei of cells that accumulated γH2AX (Supplementary Figure 4). As a positive control, sections from normal testis that had been irradiated were analyzed in parallel and in contrast, these demonstrated robust co-localization of p53 with γH2AX. From these findings, it may be concluded that the inactivation of Huwe1 in the differentiating spermatogonia led to an activation of the DDR and death through p53-independent apoptosis, thus preventing their progression into the meiotic program.

Huwe1 is not essential for meiotic progression. Huwe1 is highly expressed in pachytene spermatocytes³⁰. Interestingly, when we stained chromosome spreads of meiotic cells from the WT testis with anti-Huwe1 antibody, we found that Huwe1 was localized to the telomere ends of autosomes of pachytene spermatocytes and to the sex body, both regions of gene silencing (Fig. 5a). Histone H2A ubiquitination has been suggested to be important for meiotic sex chromosome inactivation (MSCI)^{31–33}, and so we hypothesized that Huwe1 may regulate H2A and therefore be important for meiotic progression by regulating events such as MSCI in the pachytene spermatocytes. As we observed drastic loss of pre-meiotic germ cells with our previous models, we crossed hemizygous *Spo11-Cre* males with *Huwe1^{lox/lox}* females to inactivate Huwe1 in spermatocytes that have initiated meiosis³⁴. Driven by *Spo11* promoter, the Cre recombinase expression begins at 7 dpp in the leptotene spermatocytes³⁴. Excision of the lox-P flanked region was confirmed by RT-PCR of whole testes RNA (Supplementary Figure 2). A fertility assay comparing the two genotypes revealed that the WT and *Huwe1^{-Y} Spo11-Cre* (hereafter referred to as the *Spo11-Cre* KO) males had normal fertility (Supplementary Table S1). The histology of the testis of the *Spo11-Cre* KO was similar to that of the WT with no apparent defects in spermatogenesis as indicated by the presence of spermatids in the lumen of the seminiferous tubules (Fig. 5b). The epididymal sperm number and motility in the *Spo11-Cre* KO were normal (Supplementary Figure 5). To study meiotic progression more precisely, we prepared dissociated cell spreads from testes at 28 dpp. The spreads were stained with antibody to SYCP3, a component of the axial element which gives rise to the lateral element of the synaptonemal complex between homologous chromosome pairs, and with anti-γH2AX antibody, which labels the double strand breaks in leptotene and zygotene and the sex body in pachytene and diplotene spermatocytes³⁵. Quantification of the different cell types did not reveal any significant defect in meiotic progression in the *Spo11-Cre* KO (Fig. 5c). Interestingly, the *Spo11-Cre* KO testis had a significantly higher percentage of spermatocytes that retained γH2AX on the autosomes in the pachytene and diplotene spermatocytes (where normally γH2AX is found only on the XY body) (Fig. 5c). However, this accumulation did not appear to lead to higher levels of apoptosis (Fig. 5d).

To explore if Huwe1 plays a role in MSCI, we studied the exclusion of transcriptional machinery from the XY body, one of the hallmarks of the process³⁶. RNA polymerase II staining was absent from the XY body in the *Spo11-Cre* KO as in the WT indicating normal decrease in transcription on the sex chromosomes (Fig. 5e). To further explore for effects of Huwe1 deficiency on MSCI, we examined the expression levels of several sex-linked genes (*Ube1x*, *Atp7A*, *Gla*, *Chic1* on the X chromosome and *Ube1y*, *Rbmy*, *Zfy1*, *Zfy2* on the Y chromosome) (Fig. 5f). None were significantly altered between the two groups confirming that Huwe1 does not play an essential role in MSCI. Thus, the inactivation of Huwe1 in spermatocytes does not have significant consequences on the process of meiosis.

To further confirm that Huwe1 is not important in post-meiotic development during spermatogenesis, we crossed hemizygous *Prm-Cre* males with *Huwe1^{lox/lox}* females to inactivate Huwe1 in the haploid spermatids^{37,38}. We observed no significant differences in the sperm number and motility, and testis weights between the WT

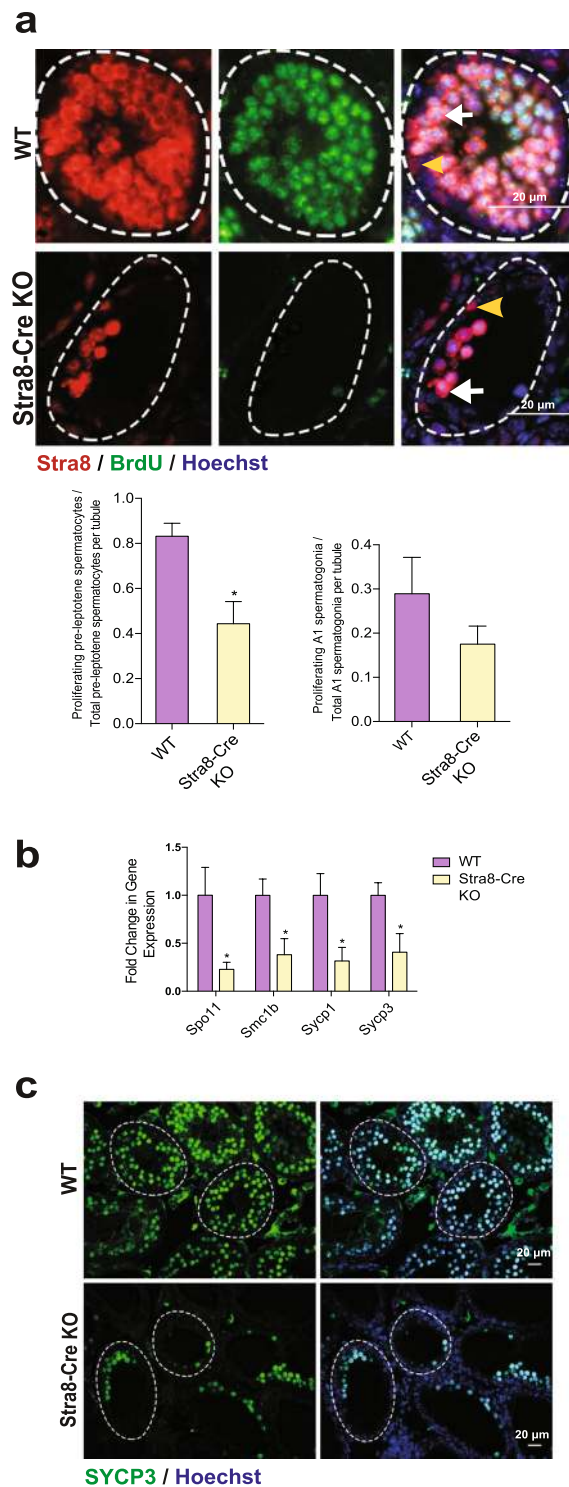


Figure 3. Huw1 is important for entry into meiosis. **(a)** Inactivation of Huw1 in the differentiating spermatogonia leads to a defect in proliferation. Representative immunofluorescence images of synchronized 8 dpRA WT and Stra8-Cre KO testis stained for Stra8 (red) and BrdU (green) (top panel). Stra8 + cells at the basement membrane of tubule are A₁ differentiating spermatogonia; Stra8 + cells away from the basement membrane are pre-leptotene spermatocytes. The yellow arrowhead indicates an A₁ differentiating spermatogonium and the white arrow indicates a pre-leptotene spermatocyte. Quantification from these images (bottom panel) WT, n = 5 (135 tubules), Stra8-Cre KO, n = 7 (271 tubules). Scale bar = 20 μm. **(b)** Expression of meiotic markers is decreased in the Stra8-Cre KO 8 dpRA testes. Q-PCR analysis of markers of meiosis (*Spo11*, *Smc1b*, *Sycp1*, *Sycp3*) on WT and Stra8-Cre KO 8 dpRA testes (WT, n = 5, Stra8-Cre KO, n = 6). **(c)** Disrupted formation of leptotene spermatocytes in Stra8-Cre KO 8 dpRA testes. Representative immunofluorescence images from WT and Stra8-Cre KO testis sections stained for SYCP3 (green). Scale bar = 20 μm. Data are shown as mean ± SEM. Student's t-test. *p < 0.05.

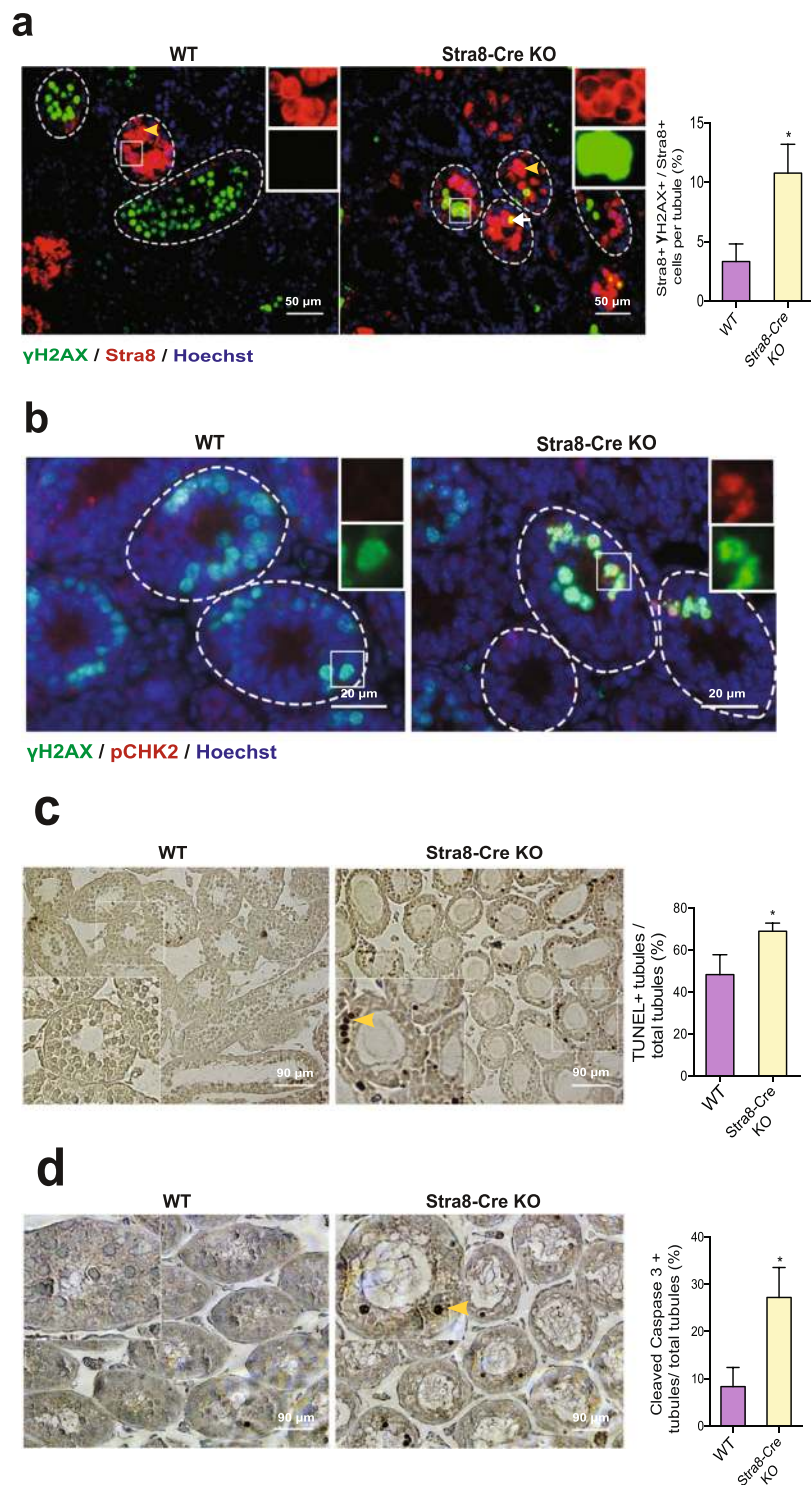


Figure 4. Inactivation of Huw1 in the differentiating spermatogonia leads to an activation of DDR and apoptotic cell death. **(a)** Loss of Huw1 resulted in elevated proportion of Stra8+ cells showing intense γ H2AX foci in unsynchronized 10 dpp testis. Representative immunofluorescence images from unsynchronized 10 dpp WT and Stra8-Cre KO testes stained for γ H2AX (green) and Stra8 (red) (left panel). γ H2AX+ Stra8+ cells in the tubules are germ cells in early meiosis (leptotene/zygotene). The yellow arrowheads indicate Stra8+ differentiating spermatogonia/pre-leptotene spermatocytes and the white arrow indicates a Stra8+ cell that is also γ H2AX+. Quantification of the proportion of Stra8+ cells that are γ H2AX+ from the images (right panel) WT, n = 4 (89 tubules), KO, n = 4 (128 tubules). Scale bar = 50 μ m. **(b)** Inactivation of Huw1 leads to the recruitment of pCHK2 to the intense γ H2AX foci in unsynchronized 10 dpp testis. Representative images from immunofluorescence staining of 10 dpp WT and Stra8-Cre KO testes stained for γ H2AX (green) and pCHK2 (red). Scale bar = 20 μ m. **(c)** Loss of Huw1 in the differentiating spermatogonia resulted in increased levels of apoptosis in the synchronized 8 dpRA testes. Shown are typical images from TUNEL assay performed on testes

sections at 8 dpRA (left panel). The yellow arrowheads indicate apoptotic cells. Scale bar = 90 μ m. Quantification from the images (right panel). WT, n = 5 (783 tubules) *Stra8*-Cre KO, n = 7 (1099 tubules). **(d)** Loss of *Huwe1* resulted in an elevated percentage of cleaved caspase 3 positive tubules in the synchronized 8 dpRA testes. Shown are typical IHC images for cleaved caspase 3 in 8 dpRA WT and *Stra8*-Cre KO testes (left panel). The yellow arrowhead indicates a cleaved caspase 3 positive cell. Scale bar = 90 μ m. Quantification from the images (right panel) WT, n = 4 (269 tubules), KO, n = 4 (286 tubules). Data are shown as mean \pm SEM. Student's t-test. * $p < 0.05$.

and *Prm*-Cre KO mice (data not shown). Histological evaluation of the testes sections revealed no evidence of impaired spermatogenesis in the *Prm*-Cre KO (data not shown). Thus, we can conclude that *Huwe1* does not play an essential role in post-meiotic development during spermatogenesis.

Discussion

In this report, we have inactivated the *Huwe1* gene at key stages during spermatogenesis to conduct a thorough evaluation of the roles of this ubiquitin ligase in the differentiation of male germ cells. For the first time, we have shown that *Huwe1* plays a critical role in the early steps of spermatogonial differentiation and entry into meiosis. Activating *Cre* recombinase in differentiating spermatogonia using the *Stra8* promoter resulted in degeneration of these cells as well as impaired replication and formation of pre-leptotene spermatocytes (Figs 2 and 3). However, *Huwe1* is dispensable for the completion of meiosis and for spermatid maturation since activating *Cre* recombinase in leptotene spermatocytes or elongating spermatids using the *Spo11* or *Prm* promoters respectively had no effects on spermatogenesis or fertility (Fig. 5 and data not shown).

The depletion of differentiating spermatogonia and preleptotene cells upon loss of *Huwe1* was associated with a hyperactivation of the DDR, revealed by the presence of intense foci of accumulation of γ H2AX in these germ cells. Although we previously observed a similar accumulation of γ H2AX in spermatogonial progenitors when *Huwe1* was inactivated in gonocytes¹⁸, there are several significant differences between the two conditions. Most importantly, the triggering of the DDR in the differentiating cells did not lead to mitotic catastrophe as we observed in the progenitors, but instead led to death by apoptosis (Fig. 4). In addition, mechanisms downstream of recruitment of γ H2AX to the sites of DNA damage were impaired in differentiating spermatogonia lacking *Huwe1*. Accumulation of ubiquitin in the γ H2AX containing foci was noticeably absent (Supplementary Figure 3). This contrasts with the normal accumulation of ubiquitinated proteins to γ H2AX foci in spermatogonial progenitors when *Huwe1* was inactivated in gonocytes¹⁸. Thus, this defect in the downstream DDR may have led to excessive activation of the upstream signaling and activation of apoptosis. At this time, we cannot rule out other possible explanations for the different responses. For example, it remains possible that the spermatogonial progenitors and differentiating spermatogonia express different activities of their apoptotic machinery with progenitors having a less active or incomplete machinery and therefore unable to couple the DDR to an apoptotic pathway. Indeed, the mitotically quiescent SSCs have been shown to be more resistant to low doses of irradiation compared to differentiating spermatogonia, also suggesting a tighter coupling of signaling in differentiating spermatogonia that leads to apoptosis³⁹. Further studies will be required to delineate the mechanisms more precisely.

Interestingly, although inactivation of *Huwe1* in leptotene spermatocytes did not exert any evident effect on spermatogenesis, it still led to accumulation of γ H2AX (Fig. 5). This accumulation was less marked than that observed in differentiating spermatogonia and was found on autosomes in pachytene and early diplotene spermatocytes, sites of double strand breaks induced during meiotic recombination. This was not associated with any apparent defect in spermatocyte development and would be consistent with the notion that the degree of hyperactivation of the DDR may be important in determining the cellular response. The modest hyperactivation seen here may have allowed resolution of the DDR in contrast to the extreme hyperactivation seen when *Huwe1* was inactivated in less differentiated cells.

We found that inactivation of *Huwe1* at three different developmental time points – gonocytes, differentiating spermatogonia and spermatocytes – led to accumulation of γ H2AX. We previously showed that inactivation of *Huwe1* in primary spermatogonia led to accumulation of also the non-phosphorylated precursor H2AX and that the accumulation of γ H2AX is due, at least in part, to the increased availability of the precursor protein. All of this is consistent with *Huwe1* targeting H2AX for ubiquitination and degradation as has been demonstrated in fibroblasts⁴⁰. It is possible that other ubiquitin ligases exist for H2AX or γ H2AX and may be active in spermatocytes, thereby limiting the increase in γ H2AX seen upon loss of *Huwe1* in these cells. Such alternative, redundant mechanisms for degrading H2AX, γ H2AX could also explain the lack of a significant phenotype upon inactivation of *Huwe1* in meiosis or spermiogenesis.

Huwe1 is a large protein having a wide array of substrates that have been characterized at a cellular level, but the physiological functions of *Huwe1* *in vivo* remain poorly characterized. Of the limited functions currently known, several of these involve modulation of tissue specific stem cells. In both neural⁴¹ and hematopoietic⁴² development, *Huwe1* suppresses proliferation of stem cells by targeting N-myc, a vital transcriptional regulator that promotes progression through the cell cycle. Loss of *Huwe1* in these tissues promotes proliferation, differentiation and exhaustion of the stem cell pool. In contrast, our current results together with those of our recent report¹⁸ indicate an opposite effect of loss of *Huwe1* on cell growth and instead identify novel, critical roles for *Huwe1* in the maintenance and differentiation of spermatogonial stem cells and associated progenitors. These roles are distinct from those in the neural and hematopoietic lineages as *Huwe1* appears to target a different substrate and the loss of *Huwe1* results not in hyperproliferation, but in impaired cell division due to hyperactivation of the DDR. Thus, *Huwe1* performs vital functions in modulating DNA repair and thereby plays a critical

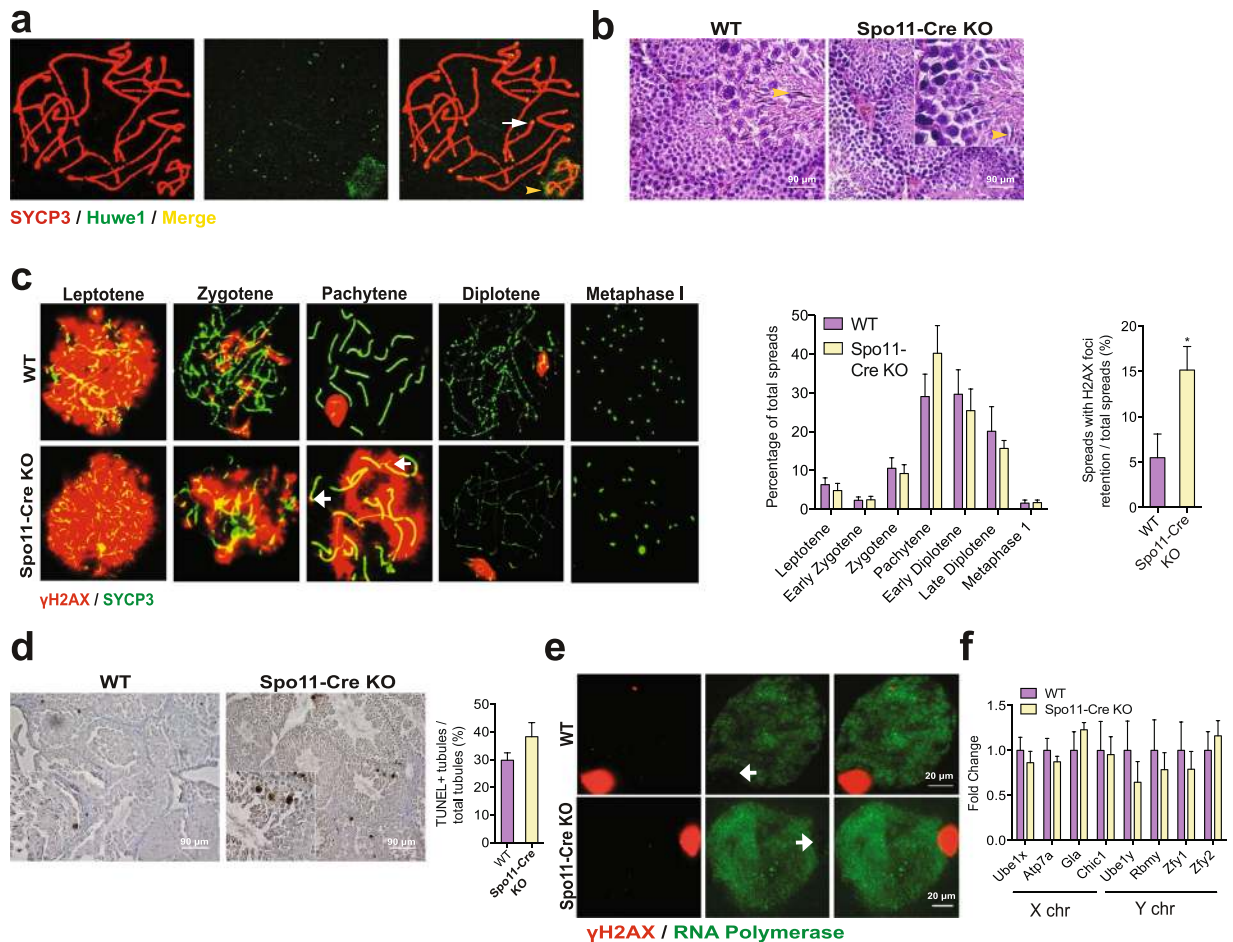


Figure 5. Huwe1 is not essential for completion of the later stages of meiosis. **(a)** Huwe1 is localized to the sex body and telomeres in pachytene spermatocytes. Representative immunofluorescence image from a chromosome spread prepared from a WT testis at 28 dpp stained for Huwe1 (green) and SYCP3 (red). White arrow points to a Huwe1 + telomere end, yellow arrowhead points to the Huwe1 + sex body. Scale bar = 20 μ m. **(b)** The Spo11-Cre KO animals have normal spermatogenesis. Hematoxylin and eosin stained testicular tissue sections from adult WT and Spo11-Cre KO. The yellow arrowheads indicate spermatids in the lumen of the seminiferous tubules. Scale bar = 90 μ m (top panel). **(c)** The Spo11-Cre KO mice show the retention of γ H2AX on the autosomes after homologous recombination. Representative immunofluorescence images of chromosome spreads prepared from WT and Spo11-Cre KO testes at 28 dpp stained for γ H2AX (green) and SYCP3 (red) (left panel). White arrow indicates γ H2AX foci on an autosome of a pachytene spermatocyte, an abnormality significantly more common in the Spo11-Cre KO testes. Quantification of different cell types from the images and of retention of γ H2AX (right panel) WT, n = 4 (402 spreads), Spo11-Cre KO, n = 6 (613 spreads). **(d)** Spo11-Cre KO of Huwe1 did not lead to increased apoptosis. Shown are typical images from TUNEL assay performed on adult testes sections of WT and Spo11-Cre KO testes (left panel). Scale bar = 90 μ m. Quantification from images (right panel) WT, n = 4 (335 tubules), KO, n = 4 (466 tubules). **(e)** RNA polymerase II remains excluded from the XY body of the Spo11-Cre KO spermatocytes. Representative immunofluorescence images of chromosome spreads prepared from WT and Spo11-Cre KO testes at 28 dpp stained for γ H2AX (red) and RNA polymerase II (green) (n = 5). The white arrows indicate the absence of RNA polymerase II stain on the XY body. Scale bar = 20 μ m. **(f)** Normal meiotic sex chromosome inactivation (MSCI) in the Spo11-Cre KO mice. Q-PCR measurements of mRNA levels of selected X-linked and Y-linked genes (n = 5). Data are represented as mean \pm SEM. Student's t-test. *p < 0.05.

role in maintaining genomic stability during the proliferation of spermatogonia, which is essential for normal spermatogenesis.

Methods

All procedures were carried out in accordance with the regulations of the Canadian Council for Animal Care and were approved by the Animal Care Committee of the McGill University Health Centre Research Institute.

Animals. Conditional Huwe1 knockout (*Huwe1^{flox/flox}*) mice were kindly provided by Drs. Antonio Iavarone and Anna Lasorella^{41,43}. To inactivate Huwe1 specifically in the differentiating spermatogonia, spermatocytes

| Gene name | | Experiment | Sequence 5' - 3' |
|--------------------|---|-------------------|-------------------------|
| Stra8 | F | QPCR | CATCATCACTGGGTTGGTTG |
| | R | QPCR | CTGCGTGTTCACAAGTGTC |
| Dazl | F | QPCR | TCCTTGACTTGTGGTTGCTG |
| | R | QPCR | CCACCTTCGAGGTTTACCA |
| Sohlh2 | F | QPCR | CCGTGCTTTTGGCTGCTAAC |
| | R | QPCR | TCACTGAAACTAATGTCAGCTCC |
| Spo11 | F | QPCR | TGCTTTGTCACTGGGATCAA |
| | R | QPCR | TACGGATCCATGTCCATGTC |
| Smc1b | F | QPCR | CATGAGGGAAAACGTCAGCAG |
| | R | QPCR | TGACACAGATCAAGCAGTCTTC |
| Sycp1 | F | QPCR | TGTCCAGTCGGGAAAACATTG |
| | R | QPCR | AGAATTAGCAACCTGTTCCGAGC |
| Sycp3 | F | QPCR | AGCCAGTAACCAGAAAATTGAGC |
| | R | QPCR | CCACTGCTGCAACACATTCATA |
| Cre Spo11/Prm-Cre) | F | PCR | CCAGGCTAAGTGCCTTCTCTACA |
| | R | PCR | AATGCTTCTGTCCGTTTGCCGGT |
| Cre (Stra8-Cre) | F | PCR | GTGCAAGCTGAACAACAGGA |
| | R | PCR | AGGGACACAGCATTGGAGTC |
| Huwe1 | F | Genotyping RT-PCR | GGCCTAGTTTATCTGCTTG |
| | R | Genotyping RT-PCR | GGATGGCCAATAGTAGCATG |

Table 1. Oligonucleotide information.

or spermatids, *Huwe1^{fllox/fllox}* females were bred with male mice hemizygous for *Stra8-Cre* (Tg(*Stra8-Cre*)1Reb)¹⁹ (Jackson Laboratory), *Spo11-Cre*²⁰ (kindly provided by Dr. Paula Cohen) or *Prm-Cre*³⁷ (Jackson Laboratory) respectively. *Huwe1^{fllox/Y}* (WT), *Huwe1^{-Y} Stra8-Cre*, *Huwe1^{-Y} Spo11-Cre*, and *Huwe1^{-Y} Prm-Cre* (KO) male offspring were identified by genomic PCR on tail DNA using oligonucleotides derived from the *Cre* recombinase sequence (Table 1).

To measure cell proliferation *in vivo*, mice were injected intraperitoneally with 50 µg/g BrdU in saline and sacrificed 24 hr later. Testes were isolated, fixed and stained as described below.

Synchronization of the seminiferous tubules was achieved as previously described²³. Briefly, 2 dpp mice were pipette fed 100 µg/g bodyweight of WIN 18446 (Tocris Bioscience), an inhibitor of retinaldehyde dehydrogenase enzyme, which is required for retinoic acid synthesis), suspended in 1% gum tragacanth (Sigma-Aldrich Canada) for 7 consecutive days. As retinoic acid is essential for spermatogonial differentiation, this treatment maintained the spermatogonia in an undifferentiated state. To initiate synchronous differentiation in all the tubules, the mice were given a subcutaneous injection of 100 µg retinoic acid (Sigma-Aldrich #R2625, Canada) diluted in 10 µl of DMSO at 9 dpp. Animals were sacrificed at the indicated times.

Analysis of sperm number and motility. For determination of sperm number, caudae epididymes were isolated from WT and KO mice, poked with a 27-gauge needle and placed in 2 ml of pre-warmed Hanks medium M199 (Invitrogen Canada Inc.). The spermatozoa were allowed to swim out for 10 min on a small plate maintained at 37 °C. Sperm were counted using a hemocytometer. For analysis of sperm motility, caudae epididymes were treated as above, but incubated in media supplemented with 3 mg/ml BSA⁴⁴. Total and progressive sperm motility were evaluated at 37 °C using a computer-assisted sperm analysis system (CASA) with Sperm Vision HR software version 1.01 (Minitube, Ingersoll, ON, Canada). For analysis of motility, a total of 200 spermatozoa were examined for each sample and the percentages of sperm total and progressive motility were analyzed.

Preparation of chromosome spreads. Glassware was washed thoroughly with ammonium hydroxide solution (Windex) followed by warm tap water and double distilled water to remove any contamination of grease. Chromosome spreads for immunofluorescence staining were obtained from 28-day old mice, a time at which the WT mice were expected to have completed meiosis in the first wave of spermatogenesis. Spreads were prepared as described⁴⁵ with modifications. The testes were isolated in MEM media with Hanks salts (MEMH) and their tunica removed. The tubules were rinsed in MEMH in a petri dish and minced with a razor blade. They were then squeezed with a pair of forceps following which they were transferred to a microfuge tube and allowed to stand in MEMH media. The media was aspirated away from the tissue and spun at 300 g for 3 min. The supernatant was removed and the cell pellet gently resuspended in residual MEMH. The cell suspension (2–3 µl) was expelled through a 20 µl micropipette on to the convex surface of 0.5% NaCl solution (completely filling a 60 mm petri dish) and allowed to spread. Following this, the spread cells were picked up by lowering a glass slide flat on the solution surface for 10 sec and fixed by placing the slide in 2% paraformaldehyde. The slides were washed in 0.4% Photo-Flo solution, dried at room temperature and stained as described below.

Tissue preparation, histology, immunostaining and TUNEL assay. Testes were fixed in 4% paraformaldehyde. For histological analysis, 4 µm sections were prepared from paraffin-embedded testes samples

| Protein name | Company | Catalog # | Conc. for immunostaining |
|-------------------|---|-------------------|--------------------------|
| Stra8 | Dr. Griswold, Washington State University | NA | 1:2000 |
| BrdU | Roche | 11 170 376 001 | 1:50 |
| γ H2Ax | Abcam | ab11174 | 1:2000 |
| γ -H2Ax | EMD Millipore | 05-636 | 1:500 |
| Sycp3 | Abcam | ab15093 | 1:100 |
| FK2 | EMD Millipore | 04-263 | 1:100 |
| pCHK2 | Cell Signaling Technology | 2661 S | 1:100 |
| Cleaved Caspase 3 | Cell Signaling Technology | 9661 | 1:100 |
| p53 (phospho S15) | Abcam | ab1431 | 1:50 |

Table 2. Antibody information.

and stained with hematoxylin and eosin. For immunofluorescence staining, the sections were rehydrated followed by antigen retrieval performed by microwaving in 10 mM citrate buffer (pH 6.0) for 6 min (maximum power). The slides were allowed to stand in the buffer for 2 min and then microwaved again for 10 min (60% power). Sections were then blocked using 10% goat serum and 1% BSA. Primary antibody (Table 2) incubation was carried out at 4 °C overnight in PBS containing 1% BSA, 2% goat serum and 0.02% Triton X-100. The next day, the sections were incubated for 2–4 hrs with appropriate secondary antibodies diluted in PBS with 1% BSA and 0.01% Triton X-100. For immunofluorescence staining of chromosome spreads, the slides were stained using the above protocol excluding the steps of rehydration and antigen retrieval. Sections were counterstained with Hoechst (Sigma, H6024), mounted with ProLong Gold antifade (Life Technologies, P36930) and examined using a Zeiss Axiovert 200 microscope. Metamorph software (version 6.3r7) was used to capture the images. Immunohistochemical staining was performed using the Vectastain ABC kit. TUNEL assay was carried out using the ApopTag Plus Peroxidase *In Situ* Apoptosis Detection Kit (Millipore, S7101). The slides were mounted with Clear-Mount (Electron Microscopy Sciences, 17985–12) and images captured on a Zeiss Axioscop 2 microscope using AxioVision Rel. 4.8 software. The slides were coded to blind the observer to the experimental condition during quantification.

RT-PCR and quantitative PCR. Total RNA was extracted from mouse testes using TRIzol reagent (Invitrogen). cDNA was synthesized from 1 μ g of RNA using the High Capacity cDNA Reverse Transcription Kit (Applied Biosystems). Primers used for RT-PCR and qPCR are shown in Table 1. QPCR was performed using Power SYBR[®] green PCR master mix in a ViiA7 qPCR analyzer (Applied Biosystems). Expression of genes was normalized to GAPDH. Differential expression was represented as fold change ($2^{-\Delta\Delta CT}$).

Statistical analysis. All statistical analysis was carried out using GraphPad Prism version 6.0 (GraphPad Software). The unpaired Student *t*-test was used to analyze the results. $P < 0.05$ was considered as significant. The numbers of animals and tubules/chromosome spreads assessed per animal have been indicated in the figure legends.

Data Availability. All data that has not been included in this research article will be made available upon request to the corresponding author.

References

- de Rooij, D. G. Stem cells in the testis. *Int. J. Exp. Pathol.* **79**, 67–80 (1998).
- Griswold, M. D., Hogarth, C. A., Bowles, J. & Koopman, P. Initiating meiosis: the case for retinoic acid. *Biol. Reprod.* **86**, 35, <https://doi.org/10.1095/biolreprod.111.096610> (2012).
- Huckins, C. The spermatogonial stem cell population in adult rats. I. Their morphology, proliferation and maturation. *Anat. Rec.* **169**, 533–557 (1971).
- Oakberg, E. F. Spermatogonial stem-cell renewal in the mouse. *Anat. Rec.* **169**, 515–531 (1971).
- Baudat, F., Manova, K., Yuen, J. P., Jasin, M. & Keeney, S. Chromosome synapsis defects and sexually dimorphic meiotic progression in mice lacking Spo11. *Mol. Cell* **6**, 989–998 (2000).
- Rathke, C., Baarends, W. M., Awe, S. & Renkawitz-Pohl, R. Chromatin dynamics during spermiogenesis. *Biochim. Biophys. Acta* **1839**, 155–168 (2014).
- Choi, Y. *et al.* Mutations in SOHLH1 gene associate with nonobstructive azoospermia. *Human Mutat.* **31**, 788–793 (2010).
- Song, B. *et al.* Association of genetic variants in SOHLH1 and SOHLH2 with non-obstructive azoospermia risk in the Chinese population. *Eur. J. Obstet. Gynecol. Reprod. Biol.* **184**, 48–52 (2015).
- Schrans-Stassen, B. H., Saunders, P. T., Cooke, H. J. & de Rooij, D. G. Nature of the spermatogenic arrest in *Dazl* $-/-$ mice. *Biol. Reprod.* **65**, 771–776 (2001).
- Yoshinaga, K. *et al.* Role of c-kit in mouse spermatogenesis: identification of spermatogonia as a specific site of c-kit expression and function. *Development* **113**, 689–699 (1991).
- Suzuki, H. *et al.* SOHLH1 and SOHLH2 coordinate spermatogonial differentiation. *Dev. Biol.* **361**, 301–312 (2012).
- Ballow, D., Meistrich, M. L., Matzuk, M. & Rajkovic, A. Sohlh1 is essential for spermatogonial differentiation. *Dev. Biol.* **294**, 161–167 (2006).
- Zhang, T., Murphy, M. W., Gearhart, M. D., Bardwell, V. J. & Zarkower, D. The mammalian Doublesex homolog DMRT6 coordinates the transition between mitotic and meiotic developmental programs during spermatogenesis. *Development* **141**, 3662–3671 (2014).
- Raverot, G., Weiss, J., Park, S. Y., Hurley, L. & Jameson, J. L. Sox3 expression in undifferentiated spermatogonia is required for the progression of spermatogenesis. *Dev. Biol.* **283**, 215–225 (2005).

15. Hao, J. *et al.* Sohlh2 knockout mice are male-sterile because of degeneration of differentiating type A spermatogonia. *Stem Cells* **26**, 1587–1597 (2008).
16. Bose, R., Manku, G., Culty, M. & Wing, S. S. Ubiquitin-proteasome system in spermatogenesis. *Adv. Exp. Med. Biol.* **759**, 181–213 (2014).
17. Liu, Z., Oughtred, R. & Wing, S. S. Characterization of E3Histone, a novel testis ubiquitin protein ligase which ubiquitinates histones. *Mol. Cell. Biol.* **25**, 2819–2831 (2005).
18. Fok, K. L. *et al.* Huwe1 regulates the establishment and maintenance of spermatogonia by suppressing DNA damage response. *Endocrinology* **158**, 4000–4016 (2017).
19. Sadate-Ngatchou, P. I., Payne, C. J., Dearth, A. T. & Braun, R. E. Cre recombinase activity specific to postnatal, premeiotic male germ cells in transgenic mice. *Genesis* **46**, 738–742 (2008).
20. Lyndaker, A. M. *et al.* Conditional inactivation of the DNA damage response gene Hus1 in mouse testis reveals separable roles for components of the RAD9-RAD1-HUS1 complex in meiotic chromosome maintenance. *PLoS Genet.* **9**, e1003320, <https://doi.org/10.1371/journal.pgen.1003320> (2013).
21. Zhao, X. *et al.* The N-Myc-DLL3 cascade is suppressed by the ubiquitin ligase Huwe1 to inhibit proliferation and promote neurogenesis in the developing brain. *Dev. Cell* **17**, 210–221 (2009).
22. Zhou, Q. *et al.* Expression of stimulated by retinoic acid gene 8 (Stra8) in spermatogenic cells induced by retinoic acid: an *in vivo* study in vitamin A-sufficient postnatal murine testes. *Biol. Reprod.* **79**, 35–42 (2008).
23. Hogarth, C. A. *et al.* Turning a spermatogenic wave into a tsunami: synchronizing murine spermatogenesis using WIN 18,446. *Biol. Reprod.* **88**, 40, <https://doi.org/10.1095/biolreprod.112.105346> (2013).
24. Monesi, V. Autoradiographic study of DNA synthesis and the cell cycle in spermatogonia and spermatocytes of mouse testis using tritiated thymidine. *J. Cell Biol.* **14**, 1–18 (1962).
25. Cohen, P. E., Pollack, S. E. & Pollard, J. W. Genetic analysis of chromosome pairing, recombination, and cell cycle control during first meiotic prophase in mammals. *Endocr. Rev.* **27**, 398–426 (2006).
26. Vergouwen, R. P. *et al.* Postnatal development of testicular cell populations in mice. *J. Reprod. Fertil.* **99**, 479–485 (1993).
27. Norbury, C. J. & Zhivotovsky, B. DNA damage-induced apoptosis. *Oncogene* **23**, 2797–2808 (2004).
28. Gown, A. M. & Willingham, M. C. Improved detection of apoptotic cells in archival paraffin sections: immunohistochemistry using antibodies to cleaved caspase 3. *J. Histochem. Cytochem.* **50**, 449–454 (2002).
29. Kamada, S., Kikkawa, U., Tsujimoto, Y. & Hunter, T. Nuclear translocation of caspase-3 is dependent on its proteolytic activation and recognition of a substrate-like protein(s). *J. Biol. Chem.* **280**, 857–860 (2005).
30. Liu, Z., Miao, D., Xia, Q., Hermo, L. & Wing, S. S. Regulated expression of the ubiquitin protein ligase, E3(Histone)/LASU1/Mule/ARF-BP1/HUWE1, during spermatogenesis. *Dev. Dyn.* **236**, 2889–2898 (2007).
31. Baarends, W. M. *et al.* Histone ubiquitination and chromatin remodeling in mouse spermatogenesis. *Dev. Biol.* **207**, 322–333 (1999).
32. Baarends, W. M. *et al.* Silencing of unpaired chromatin and histone H2A ubiquitination in mammalian meiosis. *Mol. Cell. Biol.* **25**, 1041–1053 (2005).
33. Sin, H. S. *et al.* RNF8 regulates active epigenetic modifications and escape gene activation from inactive sex chromosomes in post-meiotic spermatids. *Genes Dev.* **26**, 2737–2748 (2012).
34. Pellegrini, M. *et al.* Targeted JAM-C deletion in germ cells by Spo11-controlled Cre recombinase. *J. Cell Sci.* **124**, 91–99 (2011).
35. Mahadevaiah, S. K. *et al.* Recombinational DNA double-strand breaks in mice precede synapsis. *Nat. Genet.* **27**, 271–276 (2001).
36. Richler, C. *et al.* Splicing components are excluded from the transcriptionally inactive XY body in male meiotic nuclei. *Mol. Biol. Cell* **5**, 1341–1352 (1994).
37. O’Gorman, S., Dagenais, N. A., Qian, M. & Marchuk, Y. Protamine-Cre recombinase transgenes efficiently recombine target sequences in the male germ line of mice, but not in embryonic stem cells. *Proc. Natl. Acad. Sci. USA* **94**, 14602–14607 (1997).
38. Peschon, J. J., Behringer, R. R., Brinster, R. L. & Palmiter, R. D. Spermatid-specific expression of protamine 1 in transgenic mice. *Proc. Natl. Acad. Sci. USA* **84**, 5316–5319 (1987).
39. Rube, C. E., Zhang, S., Miebach, N., Fricke, A. & Rube, C. Protecting the heritable genome: DNA damage response mechanisms in spermatogonial stem cells. *DNA Repair (Amst)* **10**, 159–168 (2011).
40. Atsumi, Y. *et al.* ATM and SIRT6/SNF2H Mediate Transient H2AX Stabilization When DSBs Form by Blocking HUWE1 to Allow Efficient gammaH2AX Foci Formation. *Cell Rep.* **13**, 2728–2740 (2015).
41. Zhao, X. *et al.* The HECT-domain ubiquitin ligase Huwe1 controls neural differentiation and proliferation by destabilizing the N-Myc oncoprotein. *Nat. Cell Biol.* **10**, 643–653 (2008).
42. King, B. *et al.* The ubiquitin ligase Huwe1 regulates the maintenance and lymphoid commitment of hematopoietic stem cells. *Nat. Immunol.* **17**, 1312–1321 (2016).
43. D’Arca, D. *et al.* Huwe1 ubiquitin ligase is essential to synchronize neuronal and glial differentiation in the developing cerebellum. *Proc. Natl. Acad. Sci. USA* **107**, 5875–5880 (2010).
44. Slott, V. L., Suarez, J. D. & Perreault, S. D. Rat sperm motility analysis: methodologic considerations. *Reprod. Toxicol.* **5**, 449–458 (1991).
45. Peters, A. H., Plug, A. W., van Vugt, M. J. & de Boer, P. A drying-down technique for the spreading of mammalian meiocytes from the male and female germline. *Chromosome Res.* **5**, 66–68 (1997).

Acknowledgements

We thank Fazila Chouiali (Histopathology platform, The Research Institute of the McGill University Health Centre) and Marie Plourde (The Research Institute of the McGill University Health Centre) for technical assistance in preparation of paraffin-embedded slides and animal breeding respectively. The *Huwe1^{flox/flox}* mice were provided by Drs. Antonio Iavarone and Anna Lasorella and the *Spo11-Cre* mice by Dr. Paula Cohen. This research was supported by grants from the Fonds de recherche Québec–Santé/Genome Québec (#24420), the Canadian Institutes of Health Research (MOP 115106), and the Natural Sciences and Engineering Research Council of Canada (RGPIN-2016-04054) to S.S.W. and from the National Science Foundation of China to K.L.F. (81771639).

Author Contributions

Conceptualization, R.B., K.S., K.L.F. and S.S.W.; Methodology, R.B., K.S., C.F., T.T., S.S.W.; Investigation, R.B., K.S., A.R.M., G.M.; Writing – Original Draft, R.B.; Writing – Review & Editing, C.F., T.T., M.C., K.L.F. and S.S.W.; Funding Acquisition, S.S.W.; Supervision, S.S.W.

Additional Information

Supplementary information accompanies this paper at <https://doi.org/10.1038/s41598-017-17902-0>.

Competing Interests: The authors declare that they have no competing interests.

Publisher's note: Springer Nature remains neutral with regard to jurisdictional claims in published maps and institutional affiliations.



Open Access This article is licensed under a Creative Commons Attribution 4.0 International License, which permits use, sharing, adaptation, distribution and reproduction in any medium or format, as long as you give appropriate credit to the original author(s) and the source, provide a link to the Creative Commons license, and indicate if changes were made. The images or other third party material in this article are included in the article's Creative Commons license, unless indicated otherwise in a credit line to the material. If material is not included in the article's Creative Commons license and your intended use is not permitted by statutory regulation or exceeds the permitted use, you will need to obtain permission directly from the copyright holder. To view a copy of this license, visit <http://creativecommons.org/licenses/by/4.0/>.

© The Author(s) 2017